Structural basis for inhibition of complement C5 by the SSL7 protein from *Staphylococcus aureus*

Nick S. Laursen[a], Natasha Gordon[b], Stefan Hermans[b], Natalie Lorenz[b], Nicola Jackson[b], Bruce Wines[c], Edzard Spillner[d], Jesper B. Christensen[a], Morten Jensen[a], Folmer Fredslund[a], Mette Bjerre[e], Lars Sottrup-Jensen[a], John D. Fraser[b], and Gregers R. Andersen[a,1]

[a]Department of Molecular Biology, University of Aarhus, DK-8000 Aarhus, Denmark; [b]Maurice Wilkins Centre for Molecular Biodiscovery, University of Auckland, Auckland 1020, New Zealand; [c]Centre for Immunology, Burnet Institute, Melbourne, Victoria 3004, Australia; [d]Institute of Biochemistry and Food Sciences, Division of Biochemistry and Molecular Biology, University of Hamburg, 20146 Hamburg, Germany; and [e]Immunoendocrine Research Unit, Medical Research Laboratories, Aarhus University Hospital, DK-8000 Aarhus, Denmark

Edited* by Pamela J. Bjorkman, California Institute of Technology, Pasadena, CA, and approved January 11, 2010 (received for review September 21, 2009)

Staphylococcus aureus **secretes the SSL7 protein as part of its immune evasion strategy. The protein binds both complement C5 and IgA, yet it is unclear whether SSL7 cross-links these two proteins and, if so, what purpose this serves the pathogen. We have isolated a stable IgA-SSL7-C5 complex, and our crystal structure of the C5-SSL7 complex confirms that binding to C5 occurs exclusively through the C-terminal β-grasp domain of SSL7 leaving the OB domain free to interact with IgA. SSL7 interacts with C5 >70 Å from the C5a cleavage site without inducing significant conformational changes in C5, and efficient inhibition of convertase cleavage of C5 is shown to be IgA dependent. Inhibition of C5a production and bacteriolysis are all shown to require C5 and IgA binding while inhibition of hemolysis is achieved by the C5 binding SSL7 β-grasp domain alone. These results provide a conceptual and structural basis for the development of a highly specific complement inhibitor preventing only the formation of the lytic membrane attack complex without affecting the important signaling functions of C5a.**

crystallography | innate immunity | structural biology | complement | IgA

The complement system comprises >30 plasma and membrane proteins and is an essential component of innate immunity against Gram-positive bacteria such as *Staphylococcus aureus*. Complement proteins interact directly with surface molecules unique to microorganisms or alternatively to the effector region of bound antibodies. The proteolytic activation of complement results in dramatically enhanced phagocytosis (1), clearance of immune complexes and apoptotic cells (2), and mediation of inflammation (3). Complement activation also promotes adaptive immune responses by serving as a natural adjuvant, enhancing and directing responses by lymphoid cells (4, 5).

Complement activation triggers cleavage of the three homologous 185- to 200-kDa proteins C3, C4, and C5. Three activation pathways converge on C3 cleavage to C3b (6). Activation by the alternative pathway (AP) results from spontaneous hydrolysis of an internal thioester bond in C3 or by deposition of properdin on an appropriate surface (7), whereas the classical pathway (CP) and lectin-mediated pathways are activated by surface-bound immune complexes or mannan binding lectins/ficolins, respectively. Activation of the CP or the lectin pathway generates the surface-bound C3 convertase (a proteolytic enzyme cleaving C3) C4b2a, whereas the AP generates the C3 convertase C3bBb. Both may recruit an additional C3b molecule to form the CP C5 convertase C4b2a3b or the AP C5 convertase C3bBb3b (8, 9), which cleaves C5 to generate the large fragment C5b and the anaphylatoxin C5a. This binds with high affinity to the C5a receptor (CD88) on myeloid cells triggering G protein ($G\alpha_I$ and $G\alpha_{16}$)-mediated cell activation, chemotaxis, respiratory burst, and release of proinflammatory mediators (10). C5b quickly associates with C6, C7, C8, and multiple molecules of C9 to form the membrane attack complex (MAC) that results in rapid cell lysis (11). Elevated levels of C5a are implicated in a wide range of inflammatory disorders, such as rheumatoid arthritis, ischemia/reperfusion injury, sepsis, and fibrotic conditions (12). MAC deposition through C5b on erythrocytes results in destruction of these cells in the hemolytic disease paroxysmal nocturnal hemoglobinuria (PNH) (13). In addition, excessive MAC formation is linked with the pathophysiology of conditions such as antibody-mediated transplant rejection (14), inflammatory neuropathies (15) and multiple sclerosis (16).

Given its importance to innate immune clearance, pathogens have developed many strategies to prevent complement activation (17). The Staphylococcal Superantigen-Like protein 7 (SSL7) binds to C5 to inhibit complement-mediated hemolytic and bactericidal activity (18). SSL7 is bifunctional and binds to C5 and IgA Fc, thereby blocking both C5 cleavage and recognition of IgA by FcαRI (18, 19). To decipher the molecular mechanism of complement inhibition by SSL7 and to understand the functional consequences of its dual binding, we have determined the crystal structure of the C5-SSL7 complex at 3.6 Å resolution. We show that SSL7 interacts with both C5 and the cleaved C5b, and that inhibition of C5 cleavage requires the presence of IgA Fc bound simultaneously to SSL7. Our structure allows us to rationalize these results, and a detailed molecular model for the recognition of C5 by the C5 convertase is presented.

Results

Overall Structure. We determined the structure of human C5 in complex with SSL7 cloned from strain 12598 (residues 40–230 traced, 3.6 Å resolution; Table S1 and Figs. S1 and S2) or the C-terminal β-grasp domain of SSL7′ (SSL7′c) derived from strain 4227 (residues 129–230 traced, 4.2 Å resolution). Because the protein sequences of SSL7 and SSL7′ show variations in the C5 interaction region (Fig. S2), it was of interest to examine complexes with C5 of both versions of SSL7. The structures show that the C-terminal β-grasp domain in SSL7 is almost exclusively responsible for the interaction with C5 (Fig. 1 *A* and *B*), with the structures of the two complexes being essentially identical except for the absence of the OB domain in the C5-SSL7′c complex. In the C5-SSL7 complex a single electrostatic interaction is formed between E53 in the OB domain and C5 R782* (C5 residue numbers marked by *; prepro numbering used). The binding to C5 has little influence on

Author contributions: J.D.F. and G.R.A. designed research; N.S.L., N.G., S.H., N.L., N.J., J.B.C., M.J., F.F., M.B., and L.S.-J. performed research; B.W. and E.S. contributed new reagents/analytic tools; N.S.L., N.G., L.S.-J., J.D.F., and G.R.A. analyzed data; and J.D.F. and G.R.A. wrote the paper.

The authors declare no conflict of interest.

*This Direct Submission article had a prearranged editor.

Freely available online through the PNAS open access option.

Data deposition: The coordinates and structure factors for the C5-SSL7 and C5-SSL7′c complexes have been deposited in the Research Collaboratory for Structural Bioinformatics (RCSB) Protein Data Bank [IDs 3KLS (C5-SSL7) and 3KM9 (C5-SSL7′c)].

[1]To whom correspondence should be addressed. E-mail: gra@mb.au.dk.

This article contains supporting information online at www.pnas.org/cgi/content/full/0910565107/DCSupplemental.

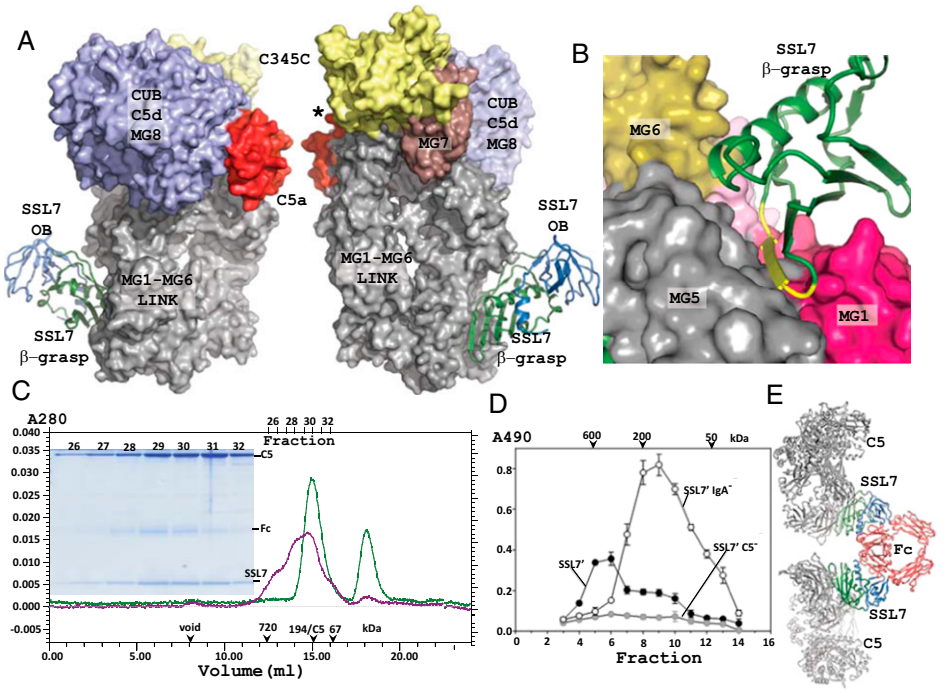

Fig. 1. The C5-SSL7 complex. (*A*) Overview of the complex with SSL7 shown in cartoon. The OB domain is colored blue and the β-grasp domain green. C5 is shown in a surface representation. In C5 the N-terminal MG1-MG6 domains and the linker region are shown in gray. The MG7 domain (brown) links the MG1-MG6 superhelix with the CUB-C5d-MG8 superdomain (blue). The flexibly attached C-terminal C345C domain is colored yellow, and the C5a domain red. In the right panel, rotated around a vertical axis relative to the left panel, the asterisk marks the position of the peptide bond cleaved by the convertase. B) Close-up on the interaction of the SSL7 β-grasp domain with three MG domains in C5. Residues 144–151 in SSL7 are colored yellow. (*C*) Superose 6 gel-filtration analysis of the C5+SSL7 (green line) and the C5+SSL7+ IgA Fc complex (magenta line). Considering the elution volume, the Fc-$SSL7_2$-$C5_2$ complex is likely to be present together with less saturated complexes. Ticks mark elution point of proteins used for calibration. (*C Inset*) Nonreducing SDS/PAGE analysis of fractions from gel filtration of C5 +SSL7+Ig A Fc. The C5+SSL7 experiment was done with excess SSL7, which elute in the peak at 18.3 mL. (*D*) Formation of SSL7-IgA-C5 complexes in human serum. Human serum was incubated with either SSL7′, SSL7′ IgA$^-$, or SSL7′ C5$^-$ and separated by gel filtration. Column fractions were tested by sandwich ELISA using plates coated with an affinity purified mouse anti-SSL7 antibody and C5 was detected with a rabbit anti-human C5 antibody. (*E*) Model of a Fc-$SSL7_2$-$C5_2$ complex with the SSL7 domains colored green or blue; Fc and C5 are colored red and gray, respectively.

the structure of SSL7 compared to the structure of the SSL7-IgA Fc complex (19) or the structure of isolated SSL7 (20). A local conformational change occurs in the loop V141-D145 within the stretch E131-L154, which is almost solely responsible for the SSL7 interaction with C5 (Figs. 1*B* and 2*A*, and Figs. S1–S3).

Likewise, relative small changes are observed in C5 (Fig. S1*B*), which at the resolution of 3.6 Å appears to be essentially unchanged relative to the structure of free C5 (21). The interaction of C5 with SSL7 is mediated mainly by the MG1 and MG5 domains with minor contributions from the MG2 and MG6 domains (Figs. 1*B* and 2*A*, and Fig. S4). Formation of the C5-SSL7 complex buries 1,919 Å^2 of surface area, which is even larger than the area of 1,568 Å^2 buried in the SSL7-IgA Fc interaction. However, the two sets of interactions are of rather different nature. In agreement with our isothermal calorimetry (ITC) measurements (Table S2 and Fig. S5), the C5-SSL7 interface (Fig. 2*A* and Fig. S3) is dominated by hydrogen bonds and electrostatic interactions, and relatively few hydrophobic interactions (PISA $\Delta^iG = -2.8$ kcal/mol), whereas the SSL7-Fc interface (19) is more hydrophobic (PISA $\Delta^iG = -5.7$ kcal/mol).

IgA-SSL7-C5 Complex. Gel-filtration analysis of combinations of pure C5, SSL7, and IgA Fc (Fig. 1*C*) show that SSL7 can bind C5 and IgA simultaneously, and strongly suggests that an Fc-$SSL7_2$-$C5_2$ pentameric complex (predicted molecular weight, 476 kDa) is formed in solution, along with the partially saturated complexes Fc-SSL7-C5 (263 kDa) and Fc-$SSL7_2$-C5 (286 kDa). To further examine the relationship between C5 and IgA binding, mutations were introduced to disrupt either or both binding sites. The SSL7′ C5$^-$ mutant contained a single charge change D147K in the β-grasp domain. The SSL7′ IgA$^-$ mutant contained three mutations (N68T.L109A.P112A) in the OB-domain that were necessary to significantly deplete IgA binding and the SSL7′ C5$^-$IgA$^-$ mutant combined all four mutations (N68T.L109A.P112A.D147K) (Fig. S6 *A* and *B*). The potential of SSL7′ to form complexes with IgA and C5 in blood was examined by incubating SSL7′, SSL7 IgA$^-$, or SSL7′ C5$^-$ with human serum followed immediately by gel filtration (Fig. 1*D*). Incubation with SSL7′ resulted in a predominant C5 containing peak eluting at ≈600 kDa consistent in size with an IgA-$SSL7'_2$-$C5_2$ pentameric complex (predicted molecular weight, 590 kDa). Incubation with the SSL7′ IgA$^-$ mutant produced a single C5 containing peak eluting at ≈200 kDa consistent in size with the SSL7′-C5 heterodimer (molecular weight, 213 kDa). The SSL7′ C5$^-$ mutant formed no detectable C5 containing complexes. The saturated pentameric complex Fc-$SSL7_2$-$C5_2$ was modeled (Fig. 1*E*) by superposition of two copies of the C5-SSL7 complex onto the Fc-$(SSL7)_2$ structure (19). This model predicts that a pentameric structure is entirely feasible with no clashes between the five molecules. The molar concentrations of IgA and C5 in blood are on the order of 10 and 0.4 μM, respectively, and so the limiting factor in the formation of this complex would be the concentration of SSL7. Notably, in the Fc-$SSL7_2$-$C5_2$ model, neither SSL7 nor IgA Fc are within 70 Å of the cleavage site at R751 in C5, suggesting that IgA forms a scaffold for SSL7 to recruit C5 in such a way as to mask a convertase binding site distant from the C5a domain.

C5-SSL7 Interface. The core of the C5-SSL7 interaction is the antiparallel pairing of the SSL7 β-strand E144-I150 and the C5 β-strand H511*-E516* with five hydrogen bonds formed between main chain atoms in the two strands (Fig. 2*A* and Figs. S2–S4). Their pairing leads to formation of a large continuous β-sheet with five strands from the inhibitor and four strands from C5. SSL7 D147 further stabilizes the interaction by electrostatic interactions with C5 R515* and by engaging in a hydrogen bond with the side chain of Y501*. SSL7 is known to strongly bind human, chimp, baboon, pig, sheep, goat, and rabbit C5, but not bovine, rat, or horse C5 (18). Sequence alignment (Fig. S4) suggests that C5 residues 511–516 are important, because this region is strictly conserved in C5 molecules that bind SSL7, whereas there are 1–3 residues with sequence variation in nonbinding C5. Hence, although this stretch forms main chain β-sheet hydrogen bonds with SSL7, even small perturbations to the C5 structure in this area can apparently lead to a significant drop in SSL7 sensitivity.

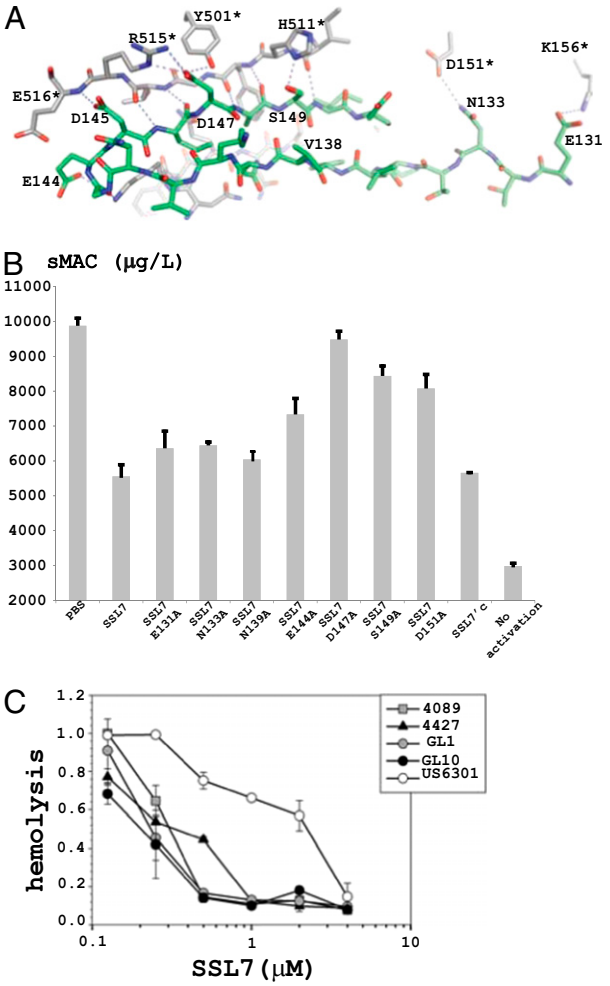

Fig. 2. The C5-SSL7 interface. (*A*) Selected atomic interactions between C5 (gray carbon atoms, * after residue number) and SSL7 (green carbon atoms). Intermolecular hydrogen bonds and electrostatic interactions are shown with dotted lines. (*B*) Inhibition of sMAC formation in serum by SSL7. (*C*) Inhibition of hemolysis with recombinant full-length SSL7 from various *S. aureus* strains. The corresponding sequences are shown in Fig. S2.

Functional and Biophysical Studies of SSL7 Mutants. The structures were validated by introducing mutations in SSL7 at residues suggested by the structures to function in C5 binding. In isothermal calorimetry (ITC) measurements (Fig. S5), wild type SSL7 formed a 1:1 complex with C5, K_d = 5.5 nM, in good agreement with SPR measurements (18). Except for the D144A mutant all other substitutions caused weaker SSL7 affinity for C5 with the most severe being the D147A and S149A mutations resulting in K_d values of 62 and 37 nM, respectively (Table S2). The same mutants were assayed for their ability to inhibit formation of soluble MAC complexes (sMAC) (22) at a fixed concentration of 0.4 μM. Full-length SSL7 inhibited sMAC formation by 63%, and all mutations resulted in weaker inhibition with substitution at D147 and S149 resulting in the largest losses (Fig. 2*B*). SSL7 D147A displayed almost no inhibition of sMAC formation, consistent with ITC results. Variations in the activities of naturally occurring alleles are also consistent with this. SSL7 from the strain US6301 was consistently a weaker inhibitor of hemolytic activity compared to four other natural alleles tested (Fig. 2*C*). SSL7 (US6301) has a histidine at position 147, whereas all other alleles have aspartic acid (Fig. S2). The sMAC assay also showed that SSL7′c was not significantly less inhibitory than full-length SSL7, indicating that IgA binding through the N-terminal OB-domain was not required to inhibit sMAC formation.

SSL7′, SSL7′ IgA$^-$, SSL7′ C5$^-$, and SSL7′c were tested by three functional assays for their ability to inhibit three complement C5-mediated functions in serum. The first assay examined the ability of SSL7 to inhibit red blood cell (RBC) hemolytic activity in 20% human or rabbit serum using alternative pathway complement activation (Fig. 3 *A* and *B*). Native SSL7′ strongly inhibited both human (IC_{50} = 0.05 μM) and rabbit (IC_{50} = 0.5 μM) serum hemolytic activity. The 10-fold difference between species in part reflects the significantly higher concentration of C5 in rabbit serum. A mutation at D147A substantially reduced SSL7 inhibition and a charge change to lysine in SSL7′ C5$^-$ resulted in complete loss of inhibition in both species (Fig. 3 *A* and *B*). Notably, inhibition profiles for both SSL7′ IgA$^-$ and SSL7′c were essentially superimposed on native SSL7′ for both species clearly indicating that IgA binding was not required to inhibit hemolysis. The second assay examined the ability of SSL7 to inhibit cell-free serum killing of a sensitive Gram-negative bacteria (Fig. 3*C*). The addition of 5% human serum to *Escherichia coli* (K12) resulted in 99.9% killing and this was strongly inhibited by the addition of native SSL7′. Bacteria killing was clearly mediated by C5 because SSL7 mutants defective in C5 binding (SSL7′ D147A, SSL7′ C5$^-$ and SSL7′ C5$^-$IgA$^-$) displayed a complete loss of function in this assay. Surprisingly, SSL7′ IgA$^-$ and SSL7′c displayed almost no inhibition (7.5% and 1% the level of native SSL7′ inhibition, respectively) at 1 μM (Fig. 3*C*). Remarkably, even a single P112A mutation in the IgA binding site had a substantial effect (18% the level of native SSL7′ at 1 μM) (Fig. 3*C* and Fig. S6*C*). This mutant has a 30-fold lower affinity for IgA (1–35 nM) (19). Thus, in contrast to inhibition of hemolysis and sMAC formation, inhibition of bacteriolysis by SSL7 was exquisitely dependent on high-affinity binding of IgA through the OB-domain.

In the third functional assay, SSL7′ and mutants were tested for their ability to inhibit C5a production in response to heat-killed *S. aureus* in 5% human serum. The calculated IC_{50} for SSL7′ in 5% serum was 0.02 μM, and a maximal inhibition of 90% was achieved above 0.06 μM, consistent with the predicted concentration of C5 in 5% human serum of 0.02 μM (Fig. 3*D*). No significant inhibition was observed for SSL7′ C5$^-$ and SSL7′ C5$^-$IgA$^-$ at any concentration. The SSL7′ IgA$^-$ and SSL7′c mutants displayed significantly reduced inhibition (40% and 50% of maximum levels, respectively) above 0.06 μM, confirming that IgA binding contributes strongly to the blocking of C5 cleavage by convertase bound to *S. aureus*. The IC_{50} for native SSL7 (allele 4427) in 100% human serum for the hemolytic assay and C5a production was calculated at 0.2–0.5 μM and did not vary significantly among a number of normal donors tested (Table S3). This is consistent with the known concentration for C5 of 0.4 μM (~75 μg/mL) and suggests that the levels of naturally occurring anti-SSL7 IgG antibodies that we have identified in most individuals do not substantially affect the ability of SSL7 to bind C5 and IgA.

Steric Hindrance and Immune Evasion. To further analyze how IgA binding to SSL7 might influence C5 cleavage, we formed a minimal and soluble C5 convertase with cobra venom factor (CVF) in complex with Bb. CVF most likely mimics the role of C3b in the AP C5 convertase and C4b in the CP C5 convertase. A high molar surplus of SSL7 in the absence of IgA decreased CVF-Bb-mediated cleavage of C5 from 74% (no SSL7) to 59% (with SSL7) after 4 h, whereas the addition of both IgA Fc and SSL7 reduced cleavage to 9% after 4 h (Fig. 4*A*).

Based on the recent structure of C3bBb-SCIN, a model was proposed for how the C3bBb and C4b2a C3 convertases recognize the C3 substrate (23). We have extrapolated this model to suggest how C5 might also be bound by the convertase without any steric clashes between the substrate C5 and the C5 convertase C3b/C4b via dimerization of the MG4-MG5 domains (Fig. 4 *B* and *C*, and Fig. S7). This model offers an explanation as to why IgA Fc is

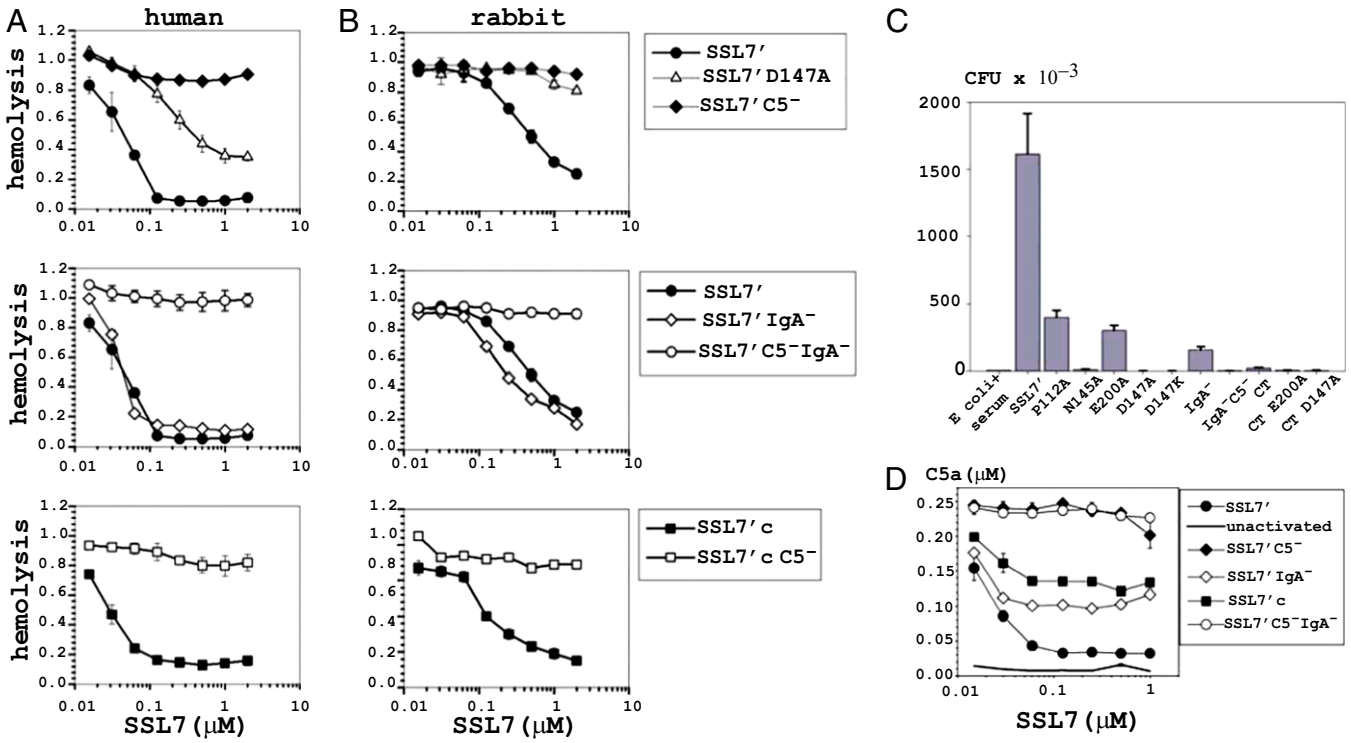

Fig. 3. Consequences of SSL7 mutants defective in C5 and IgA binding on complement C5-mediated functions. (*A* and *B*) The ability of SSL7′ and SSL7′ mutants to inhibit the hemolytic activity in 20% human serum against human red blood cells (*A*) or 20% rabbit serum against human red blood cells (*B*). These assays were performed in triplicate and represent the results from a single representative donor. Equivalent results were achieved from multiple donors. (*C*) Inhibition by 1 μM SSL7′ and SSL7′ mutants against killing of *E. coli* by 5% human serum. Bacterial survival was enumerated by colony plating in triplicate for each dilution. Results are representative of three repeat experiments. (*D*) Inhibition by varying concentrations of SSL7′ and SSL7′ mutants of complement C5a production in response to the addition of 10^7 heat-killed *S. aureus* to 10% cell-free human serum. C5a was quantified by sandwich ELISA, using a commercial C5a as a concentration standard. The results are representative of two separate experiments from a single donor.

needed to efficiently inhibit cleavage of the C5-SSL7 complex. One SSL7 molecule bound directly to C5 does not overlap with C3b in the convertase, whereas IgA Fc bound to this SSL7 overlaps with the C3b at a single loop. A second SSL7 bound to Fc is predicted to significantly constrain the binding of C3b (Fig. 4 *B* and *C*) and a second C5 molecule bound to the second SSL7 would completely prevent convertase binding to not one but both C5 molecules captured in the complex.

We have noted another potential consequence of SSL7 cross-linking C5 and IgA. Only a single edge of the relatively flat SSL7 molecules appears to be accessible to antibody recognition once the C5-SSL7-IgA complex is formed (Fig. S8). On top of this, the affinity for C5 and IgA is so high that the concentration of neutralizing SSL7 specific IgG will have to be similarly high to achieve neutralization. A similar mechanism for evading aggregation by host antibodies may apply to other pathogen proteins that form large complexes with multiple large abundant host proteins. Several other complement inhibitor proteins from pathogens bind multiple abundant high molecular weight host proteins (24).

SSL7 Binds to C5b. The structure of C5b is unknown but may resemble C3b (25, 26), suggesting that the release of C5a triggers a major conformational change in the C5d-CUB-MG8 superdomain, leaving the MG1-MG6 superhelix largely unchanged (Fig. S9*A*). Hence, a C5b closely resembling C3b is predicted to bind SSL7. To verify this, we generated C5b with CVF-Bb and then incubated it with His-tagged SSL7. The C5b-SSL7 complex was isolated, and the strength of this intermolecular interaction appeared to be similar to that observed for the C5-SSL7 complex (Fig. S9*B*). This suggests that there are no substantial changes in packing of the MG1, MG2, and MG5 domains upon C5 cleavage, because such changes would be expected to affect SSL7 binding.

Discussion

C5 Convertase. There are now two known binding sites for pathogen proteins inhibiting cleavage of C5. OmCI appears to lock the conformation of C5 and in particular the C345C domain (21), whereas SSL7 binds at the opposite end of the molecule between the distal MG1 and MG5 domains. Both inhibitors appear to block C5 cleavage by interfering with convertase recognition far from C5a. Convertase binding seems to require surface regions distributed along the entire length of the C5. In both the AP and CP C5 convertases, an additional molecule of C3b is present in addition to the C3b/C4b and Bb/C2a. This switches the specificity from C3 to C5 by decreasing the K_m for the C5 substrate (27). This additional C3b molecule required to convert the C3 convertase to a C5 convertase is apparently not necessary for the SSL7-IgA-mediated inhibition according to our proteolysis results with the minimal CVF-Bb C5 convertase. Our model of C5 recognition by C3b/C4b is based on an interaction similar to that proposed for C3 with C3b/C4b (23), and the model explains the importance of IgA Fc in SSL7-mediated inhibition of CVF-Bb C5 cleavage. In addition, it agrees with results showing that residues centered around R462 (mature C4 numbering) in the MG5 domain of human C4b are directly involved in C5 recognition by the CP C5 convertase (28).

Inhibition Modes of SSL7. Our model of the IgA-$SSL7_2$-$C5_2$ complex (Fig. 1*E*) does not predict any direct IgA-C5 interactions. But IgA-mediated steric hindrance appears to be the most likely

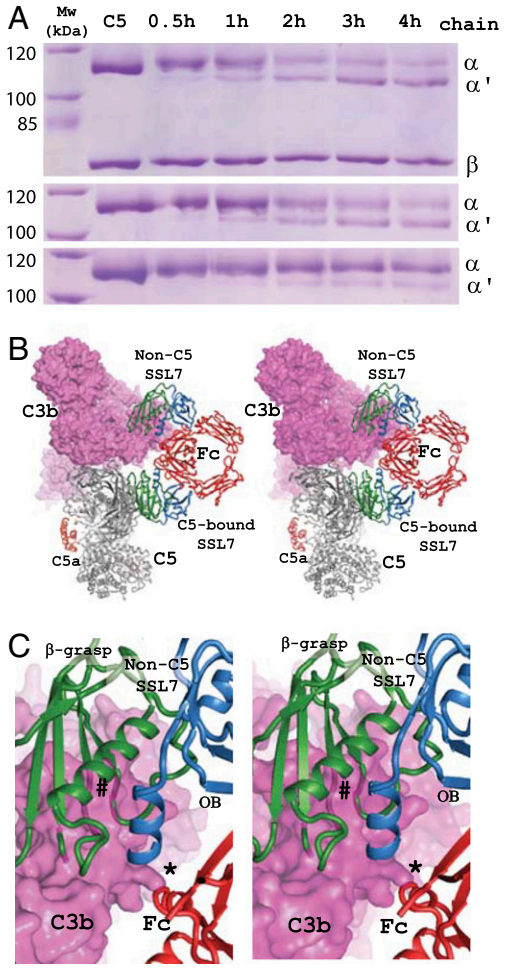

Fig. 4. The role of IgA in inhibition of C5 cleavage. (*A*) SDS/PAGE analysis of proteolytic degradation of C5 with the CVF-Bb protease. The top gel shows a time course of proteolysis in the absence of SSL7 and IgA Fc, middle gel time course in the presence of SSL7, and bottom gel in the presence of both SSL7 and IgA Fc. α and α′, position of the undigested and digested C5 α-chain, respectively; β, position of the C5 β-chain not affected by proteolysis. (*B*) Stereoview of model with C5 bound to the C3b subunit of the convertase but with the $SSL7_2$-Fc complex bound to C5. The C3b molecule of the convertase is shown as a magenta surface. (*C*) Close-up of the overlap between C5-bound $SSL7_2$-Fc and the C3b subunit of the convertase. Whereas the C5-bound SSL7 would not overlap with C3b, IgA Fc would overlap with C3b at one Fc loop (marked "*"), and the non-C5 SSL7 recruited by IgA would make a massive clash (marked "#") with C3b.

explanation for our observations concerning the IgA/Fc dependence for inhibition of C5 cleavage. However, we cannot formally exclude minor allosteric changes transmitted from the SSL7 binding site to the C5 convertase cleavage site upon binding of the inhibitor that are not apparent within the medium resolution of the structure. However such changes are likely to be insignificant relative to the changes required to expose Arg751 as previously discussed (21).

A striking outcome of the functional assays is that SSL7 distinguishes two different mechanisms of C5-mediated lysis, one for red blood cells where the β-grasp domain of SSL7 inhibits as effectively as full-length SSL7′ and another for *E. coli* bacteriolysis where even the slightest drop in IgA binding reduced SSL7 inhibition. We interpret this to mean that SSL7 inhibits at two distinct steps in the end-stage of the complement response. The first step is to block the recognition and cleavage by capturing C5 in a large complex with IgA preventing access by surface bound C5 convertase or the soluble CVF-Bb complex. The second step is blocking downstream formation of MAC complex once C5b has been formed, which is in agreement with the ability of SSL7 to bind preformed C5b and the inhibition of RBC lysis and sMAC formation by the β-grasp domain in SSL7′c. From the perspective of the Gram positive *S. aureus* which is impervious to MAC, the most likely role of SSL7 is to limit C5a production because of its critical regulatory role in the activation of phagocytosis, the main mechanism of clearance of this bacterium.

In contrast to RBC lysis by MAC, inhibition of bactericidal activity and C5a production are exquisitely dependent on IgA binding. This suggests that blocking MAC formation on its own is not sufficient to inhibit the killing of bacteria further suggesting that MAC assembly may occur differently on RBC compared to *E. coli* cells. A clue to the differential inhibition of hemolysis and bacteriolysis is found in a comparison of the three IC_{50} values. 50% inhibition of hemolysis and C5a production in whole serum (here performed in 20% and 10% serum, respectively) was 0.5 μM which is close to the serum concentration of C5 (Table S3). However the IC_{50} for bacteriolysis (performed here in 5% serum) was 10-times higher at 8 μM for complete serum. One explanation is that inhibition of the alternative pathway C5 convertase C3bBb3b (regulating hemolysis) does not require the pentameric IgA-$SSL7_2$-$C5_2$ complex, whereas the classical pathway C5 convertase C4b2a3b (regulating bacteriocidal activity) is less sensitive to SSL7 and thus demands higher concentrations of SSL7 to saturate the available IgA, thereby favoring the pentameric complex.

Why then did the β-grasp domain show partial inhibition of C5a production when IgA was completely absent from the complex? The answer may lie in the presence of naturally occurring anti-SSL7 IgG that bind epitopes in the β-grasp domain that are exposed in the absence of IgA. These may form trimeric complexes with C5-SSL7 that block convertase access similar to C5-SSL7-IgA complexes. Interestingly, the inhibition of C5a production by both SSL7′c and SSL7′-IgA^- did not increase above a concentration of 0.06 μM (Fig. 3*D*), suggesting that the anti-SSL7 IgG that substitutes for IgA had been saturated and that, above this concentration, only dimeric C5-SSL7′c was generated that blocks MAC formation but not C5 activation.

Implications for Development of Novel C5 Inhibitors. Blocking of C5 cleavage or the downstream functions of C5a or C5b represents a strategy for treating conditions uniquely associated with end-stage complement activation while preserving the essential immunoregulatory and immunoprotective roles of proximal complement activation. Eculizumab, a humanized monoclonal antibody for the treatment of PNH that prevents C5 cleavage, is the first complement inhibitor approved by the FDA and EMEA (13). SSL7, a small and easy to produce protein, may offer an alternative to expensive humanized antibodies. Moreover, the small C-terminal domain of SSL7 offers the potential to selectively block the lytic effects of MAC without affecting the essential role of C5a in regulating innate immunity. Whether or not the native SSL7 of SSL7 β-grasp domain proves useful therapeutically, it clearly identifies a crucial region on C5 to selectively target with therapeutics designed to block excessive hemolysis without affecting C5a-mediated innate immunity.

Materials and Methods

Protein Expression and Purification. Human C5 was purified as described in ref. 21. The SSL7 and SSL7′ proteins and their mutants were produced as recombinant proteins in *E. coli* and purified with affinity chromatography. Before crystallization, the C5-SSL7/C5-SSL7′ complex was purified by gel filtration. Human IgA1-Fc (C242 to P455; IgA1 myeloma Bur numbering) was expressed using a derivative of pAPEX-3p in HEK293EBNA cells as described in ref. 19. CVF was purified from lyophilized *Naja naja siamensis* venom by gel filtration.

Crystallization and Structure Determination. Crystals were obtained through vapor diffusion by mixing of 6 mg/mL protein in a 1:1 ratio with the reservoir buffer containing 50 mM $MgAc_2$ and 50 mM Mes (pH 6.2). Diffraction data were processed with XDS (29) (Table S1). The structure of C5-SSL7 was determined by molecular replacement using PHASER (30). Both models were rebuilt in O (31) and refined with PHENIX (32).

Time Course of C5 Cleavage and C5b-SSL7 Pull-Down. Convertase complexes were formed by mixing CVF, fB, and fD (Complement Technology) in a molar ratio (relative to 1 mol of C5) of 0.05:0.05:0.0015 in 20 mM Tris/150 mM NaCl/10 mM $MgCl_2$ (pH 8.0) at 37 °C for 1 h. Before cleavage, C5 alone or mixed with a 4-fold molar excess of SSL7or SSL7 + IgA-Fc was incubated at 37 °C for 1 h before mixing with the preformed convertases and digestion took place at 37 °C for up to 4 h. SSL7 pull-down experiments with C5 or C5b were done by incubating Ni^{2+}-NTA agarose with either C5-SSL7 or C5b-SSL7. The intensities of the α- and α′-chains in C5/C5b were quantified with ImageJ.

Biophysical Measurements. The ITC experiments were performed at 30 °C in a VP-ITC instrument from MicroCal and data were analyzed using the Origin software package.

Inhibition of sMAC (sC5b-9) Formation. SSL7 and SSL7 mutants (20 μM in phosphate-buffed saline) were diluted to 0.4 μM in normal human serum and incubated at 37 °C for 4 h. Sera with addition of buffer only incubated at 37 °C or 4 °C (no activation) were used as controls. The generation of sMAC was determined by an immunofluorometric assay (33), and the data in Fig. 2*B* represent the mean and standard deviation for six experiments with each SSL7 variant.

Serum Hemolytic Assay. RBCs from human or sheep (Invitrogen; Alsevers sheep blood) were combined with human and rabbit serum, respectively. The RBCs were standardized to 2×10^8 cells per mL. SSL7′ protein was added to 96-well U-bottom tissue culture plates (Falcon) to give a 2-fold dilution series and added 100 μL of diluted serum diluted with GHB (150 mM NaCl, 5 mM hepes, 0.11 (wt/vol) Gelatin from bovine skin type B)/MgEGTA. Fifty microliters of RBCs was added, and the plate was incubated for 1 h at 37 °C with periodic shaking. The cells were pelleted by centrifugation, 100 μL of the supernatant was added to 150 μL of ice-cold 150 mM NaCl in 96-well, flat-bottom tissue culture plates (Falcon), and the absorbance at 412 nm was measured using a uQuant plate reader (BioTek).

Serum Cell-Free Bactericidal Assay. Sera were allowed to coagulate, and serum was centrifuged for 5,000 × *g* for 5 min before use. Cell-free serum bactericidal activity was assessed using a fresh overnight culture of *E. coli* K12 strain DH5α. SSL7′ protein was preincubated with 5% normal human serum diluted in Hanks's buffered saline solution (HBSS) (Sigma Aldrich) for 30 min at 37 °C in borosilicate glass tubes and then incubated with $\sim 1 \times 10^7$ stationary-phase ($A_{600} \sim 0.15$) DH5α cells for 90 min at 37 °C. Tubes were placed in ice to stop reactions, and then a dilution series of each was prepared in HBSS and then plated in triplicate on LB agar and then incubated overnight at 37 °C. Colony-forming units (CFU) were enumerated the following day on a BacCount (BioTek) and expressed as mean CFU ± SD.

Detection of Serum C5a Production. One hundred-microliter samples of 25% serum were mixed with 50 μl of serially diluted SSL7 or SSL7 mutant proteins before the addition of 100 μL of PBS-BSA containing 10^7 heat-killed *S. aureus*. Plates were incubated at 37 °C for 30 min and then centrifuged for 5 min at 1,250 × *g* to pellet bacteria, and the amount of C5a formed was quantified with a C5a mAb-based sandwich ELISA.

Further details of experimental procedures are described in the *SI Materials and Methods*.

ACKNOWLEDGMENTS. We thank L. Kristensen, G. Hartvigsen, D. Wulff, H. Trist, S. Ling, and F. Clow for excellent technical assistance; the staff at the MAX-lab, European Synchrotron Radiation Facility, and Swiss Light Source beamlines for help with data collection; and K. Poulsen for *S. aureus* DNA. G. R.A. was supported by the Danish Science Research Council, Danscatt, the Vilhelm Petersen Foundation, and a Hallas-Møller stipend from the Novo Nordisk Foundation. J.D.F. was supported by the Health Research Council of New Zealand.

1. Walport MJ (2001) Complement. First of two parts. *N Engl J Med* 344:1058–1066.
2. Manderson AP, Botto M, Walport MJ (2004) The role of complement in the development of systemic lupus erythematosus. *Annu Rev Immunol* 22:431–456.
3. Guo RF, Ward PA (2005) Role of C5a in inflammatory responses. *Annu Rev Immunol* 23:821–852.
4. Carroll MC (2004) The complement system in regulation of adaptive immunity. *Nat Immunol* 5:981–986.
5. Hawlisch H, Köhl J (2006) Complement and Toll-like receptors: key regulators of adaptive immune responses. *Mol Immunol* 43:13–21.
6. Harboe M, Mollnes TE (2008) The alternative complement pathway revisited. *J Cell Mol Med* 12:1074–1084.
7. Spitzer D, Mitchell LM, Atkinson JP, Hourcade DE (2007) Properdin can initiate complement activation by binding specific target surfaces and providing a platform for de novo convertase assembly. *J Immunol* 179:2600–2608.
8. Kinoshita T, et al. (1988) C5 convertase of the alternative complement pathway: covalent linkage between two C3b molecules within the trimolecular complex enzyme. *J Immunol* 141:3895–3901.
9. Takata Y, et al. (1987) Covalent association of C3b with C4b within C5 convertase of the classical complement pathway. *J Exp Med* 165:1494–1507.
10. Klos A, et al. (2009) The role of the anaphylatoxins in health and disease. *Mol Immunol* 46:2753–2766.
11. Gasque P (2004) Complement: a unique innate immune sensor for danger signals. *Mol Immunol* 41:1089–1098.
12. Monk PN, Scola AM, Madala P, Fairlie DP (2007) Function, structure and therapeutic potential of complement C5a receptors. *Br J Pharmacol* 152:429–448.
13. Rother RP, Rollins SA, Mojcik CF, Brodsky RA, Bell L (2007) Discovery and development of the complement inhibitor eculizumab for the treatment of paroxysmal nocturnal hemoglobinuria. *Nat Biotechnol* 25:1256–1264.
14. Wang H, et al. (2005) Prevention of acute vascular rejection by a functionally blocking anti-C5 monoclonal antibody combined with cyclosporine. *Transplantation* 79: 1121–1127.
15. Lehmann HC, Hartung HP (2008) Complementing the therapeutic armamentarium for Miller Fisher Syndrome and related immune neuropathies. *Brain* 131:1168–1170.
16. Oh S, Cudrici C, Ito T, Rus H (2008) B-cells and humoral immunity in multiple sclerosis. Implications for therapy. *Immunol Res* 40:224–234.
17. Blom AM, Hallström T, Riesbeck K (2009) Complement evasion strategies of pathogens-acquisition of inhibitors and beyond. *Mol Immunol* 46:2808–2817.
18. Langley R, et al. (2005) The staphylococcal superantigen-like protein 7 binds IgA and complement C5 and inhibits IgA-Fc alpha RI binding and serum killing of bacteria. *J Immunol* 174:2926–2933.
19. Ramsland PA, et al. (2007) Structural basis for evasion of IgA immunity by Staphylococcus aureus revealed in the complex of SSL7 with Fc of human IgA1. *Proc Natl Acad Sci USA* 104:15051–15056.
20. Al-Shangiti AM, et al. (2004) Structural relationships and cellular tropism of staphylococcal superantigen-like proteins. *Infect Immun* 72:4261–4270.
21. Fredslund F, et al. (2008) Structure of and influence of a tick complement inhibitor on human complement component 5. *Nat Immunol* 9:753–760.
22. Choi NH, Nakano Y, Tobe T, Mazda T, Tomita M (1990) Incorporation of SP-40,40 into the soluble membrane attack complex (SMAC, SC5b-9) of complement. *Int Immunol* 2: 413–417.
23. Rooijakkers SH, et al. (2009) Structural and functional implications of the alternative complement pathway C3 convertase stabilized by a staphylococcal inhibitor. *Nat Immunol* 10:721–727.
24. Lambris JD, Ricklin D, Geisbrecht BV (2008) Complement evasion by human pathogens. *Nat Rev Microbiol* 6:132–142.
25. Wiesmann C, et al. (2006) Structure of C3b in complex with CRIg gives insights into regulation of complement activation. *Nature* 444:217–220.
26. Janssen BJ, Christodoulidou A, McCarthy A, Lambris JD, Gros P (2006) Structure of C3b reveals conformational changes that underlie complement activity. *Nature* 444: 213–216.
27. Rawal N, Pangburn M (2001) Formation of high-affinity C5 convertases of the alternative pathway of complement. *J Immunol* 166:2635–2642.
28. Ebanks RO, Isenman DE (1995) Evidence for the involvement of arginine 462 and the flanking sequence of human C4 beta-chain in mediating C5 binding to the C4b subcomponent of the classical complement pathway C5 convertase. *J Immunol* 154: 2808–2820.
29. Kabsch W (2001) Crystallography of biological macromolecules in XDS. *International Tables for Crystallography*, eds Rossmann MG, Arnold E (Kluwer Academic, Dordrecht, The Netherlands) Vol F, Ch 25.22.29.
30. McCoy AJ (2007) Solving structures of protein complexes by molecular replacement with Phaser. *Acta Crystallogr D Biol Crystallogr* 63:32–41.
31. Jones TA, Zou JY, Cowan SW, Kjeldgaard M (1991) Improved methods for building protein models in electron density maps and the location of errors in these models. *Acta Crystallogr A* 47:110–119.
32. Adams PD, et al. (2002) PHENIX: building new software for automated crystallographic structure determination. *Acta Crystallogr D Biol Crystallogr* 58:1948–1954.
33. Haahr-Pedersen S, et al. (2009) Level of complement activity predicts cardiac dysfunction after acute myocardial infarction treated with primary percutaneous coronary intervention. *J Invasive Cardiol* 21:13–19.